Front. Optoelectron. 2017, 10(2): 144–150
DOI 10.1007/s12200-017-0670-3

RESEARCH ARTICLE

Nested microring resonator with a doubled free spectral range for sensing application

Xin ZHANG (✉), Jiawen JIAN, Han JIN, Peipeng XU

Faculty of Electrical Engineering and Computer Science, Ningbo University, Ningbo 315211, China

© Higher Education Press and Springer-Verlag Berlin Heidelberg 2017

Abstract The microring resonator has received increasing attention in the optical sensing application because of its micro-size, optical property, and high sensitivity. An additional waveguide is commonly used to change the output spectra in the early research on microring resonators. In this study, we proposed a nested microring resonator that doubles the free spectral range (FSR) compared with the conventional single microring. This structure improved the sensing property as the FSR in the filter output spectra could be considered as a measurement range in the microring sensor. Moreover, the parameters including the coupling coefficient of the three coupling sections, length of the U-bend waveguide, and effective index of a waveguide were tested and carefully selected to optimize the sensing properties. The relationship between these parameters and the output spectra was demonstrated. With linear sensitivity, the structure has a good potential in sensing application.

Keywords microring resonator, double free spectral range (FSR), sensing application, large measurement range

1 Introduction

With the advancement of micro/nanofabrication technologies, microring resonators have become widely used in sensing application because of their filter characteristic, especially in terms of stress measurement and biochemical detection [1–6]. The parameters characterizing filter properties, namely, free spectral range (FSR), extinction ratio (ER), and bandwidth of the resonant peak/notch, describe the sensing properties of measurement range, precision, and accuracy [7]. FSR, which is the distance between two adjacent resonant notches/peaks in filter spectra, determines the measurement range of the sensor in the frequency modulation measurement [8]. ER expresses the depth of the resonant notch in the filtered spectra. In the design of microring sensors, enlarging the measurement range can cause the FSR to enlarge as well. Thus, microring sensors have received considerable attention. Studies on enlarging the FSR in a single ring are divided into two aspects: minimizing the size of a microring resonator and adding another waveguide. The first aspect relies on the precision of equipment in micro/nanofabrication. The smallest microring ever reported has a radius of 1.5 μm with 62.5 nm of FSR [9]. The U-bend waveguide is examined as an additional waveguide for FSR expansion based on the light field interference. Lu et al. and Li et al. used the U-bend waveguide in expanding FSR in 2011 and 2012, respectively [10,11]. In both works, the output light field was collected from the Through port and added to the Add port through the U-bend waveguide, and the FSR was doubled compared with the conventional add–drop structure. Structures with one piece of a U-bend waveguide could only realize a band-reject filter because two ports (Through and Add) in the add–drop structure are occupied by the U-bend waveguide, although these structures had a simple design and high Q-factor. Furthermore, the ER of the resonant notch in previous works was small, thus indicating that light detection and disturbance-resist are difficult to obtain. In these papers, ER could be enlarged by decreasing the coupling coefficient between waveguide and ring. However, a new problem of large transmission loss could be generated. Xiang et al. applied the structure of a dual microring resonator with U-bend waveguide feedback in sensing and FSR expansion [12]. This structure extends the measurement range in the weak coupling case.

In this study, we proposed a new structure of a single-ring resonator with a doubled FSR compared with the conventional add–drop filter structure. The proposed structure had a straight waveguide coupled with a U-bend waveguide, which had one nested microring inside.

Received September 29, 2016; accepted December 28, 2016

E-mail: owen88zjnbzhx@126.com

This new structure had four ports for optical communication and could realize both band-pass and band-reject filters. The output filtered spectrum of the proposed structure was optimized for enhancing the sensing properties by carefully selecting the parameters. The ER reached more than 30 dB, and the FSR was measured at 24 nm with a radius of 50 μm. Similar to the conventional add–drop structure, this structure also had a linear sensitivity curve, which shows great potential in sensing applications.

2 Device structure and spectrum simulation

The schematic of the proposed nested microring resonator is illustrated in Fig. 1(a). The microring resonator includes a single microring nested inside a piece of U-bend waveguide and a straight waveguide coupled outside. The structural parameters were selected as follows: the ring radius R was 30 μm, and the length of the U-bend waveguide was $2\pi R$ to maintain phase matching. The Lumerical FDTD Solutions and Interconnect software programs were used for simulation, and the silicon on insulator (SOI) was selected as the device material. We assumed that the waveguide loss factor was $\alpha = 1.8$ dB/cm. Figure 1(b) shows the cross-section and transmission TE mode of the structure. The SOI ridge waveguide was 450 nm in width and 220 nm in thickness. The effective refractive index of waveguide n_{eff} was 2.20. The bend loss influence on the transmission mode was ignored because the radius of the microring resonator was relatively large.

This new structure had four ports similar to the conventional add–drop structure: In, Through, Add, and Out. Figure 2 illustrates the simulated output spectra of Port Through and Port Out in a wavelength range of 1500–1600 nm and a coupling coefficient k of 0.2. The corresponding spectra of the conventional structure are also displayed for comparison. Figures 2(a) and 2(c) depict the transmission spectra in Port Through of the proposed configuration and the traditional add–drop structure, respectively. The resonant notches were depressed at the wavelengths of 1505, 1529, 1553, and 1580 nm. The other resonant notches were enlarged, and the depressed notches were consequently regarded as pseudo-modes. Thus, the FSR of the output spectrum was considered to double from 12 to 24 nm despite the pseudo-mode of the small notches. The enlarged light extinction at the resonant wavelength made the filter effect more obvious. In sensing applications based on frequency modulation, a large FSR usually means a large measurement range. In addition, the more obvious the filter effect, which includes a large extinction ratio and a thin bandwidth of the resonant notches, the better the precision and resolution are. Therefore, the sensor based on the proposed configuration should have a larger measurement range than that based on the conventional structure. In Figs. 2(b) and 2(d), the output spectra in Port Out do not double its FSR unlike the outcome in Port Through. The resonant peaks at the wavelengths of 1505, 1529, 1553, and 1580 nm became narrower than the conventional peaks, as presented in Fig. 2(d), but the ER was not small enough to be ignored compared with other peaks. The ER in Port Out spectra was observed only at approximately 1 dB, which was smaller than that of the conventional structure at 20 dB. Thus, as the filter effect in Port Out did not meet the demand of large extinction for sensing, we focused on the spectra in Port Through and discussed how this output spectrum changed with varying parameters, such as coupling coefficient k, phase shift φ, and effective index n_{eff}. We also focused on enlarging FSR and ER, decreasing bandwidth, and depressing pseudo-modes to obtain better sensing ability, as these parameters influence the output spectrum.

3 Results and discussion

We tested whether or not the output spectra of the two ports would change if Port In and Port Add were switched before

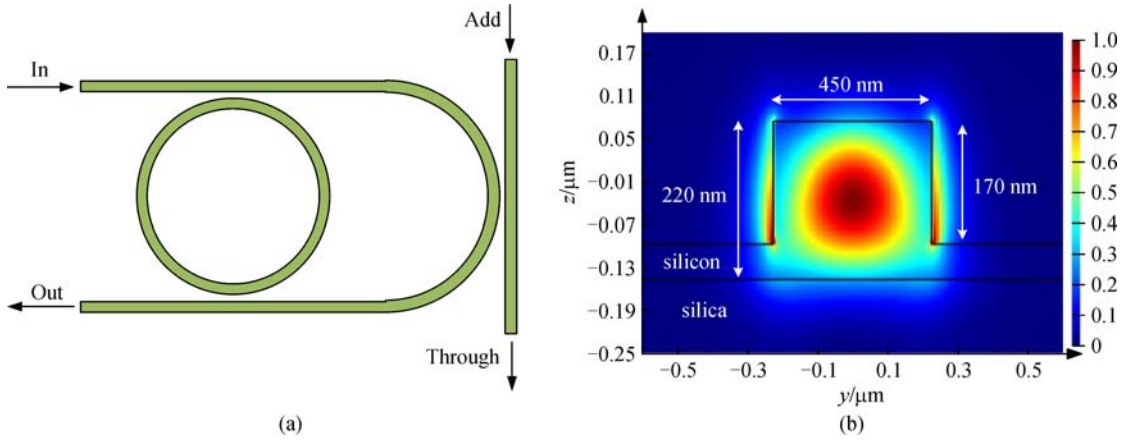

Fig. 1 Schematic of (a) the nested microring and (b) the cross-section of its waveguide

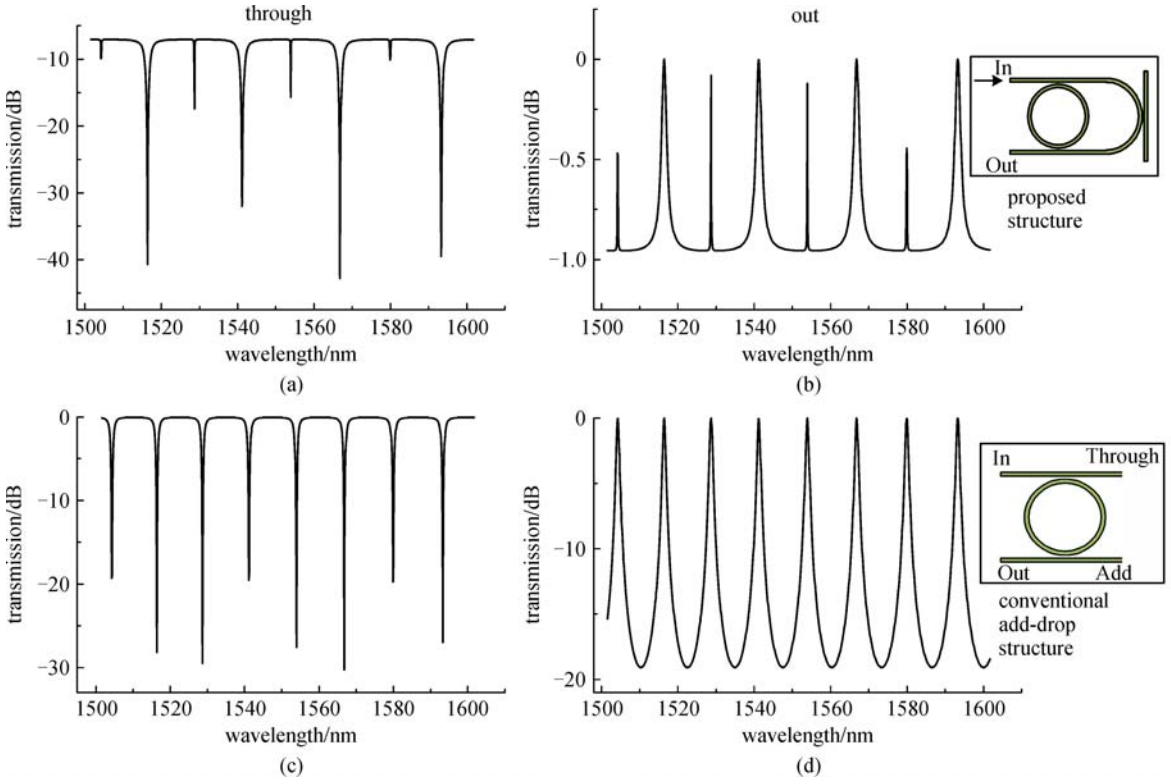

Fig. 2 Output spectra of Port Through and Port Out for the proposed structure (a) and (b) and the conventional structure (c) and (d)

changing the parameter and recording the output. The result is shown in Fig. 3. The output spectra of Port Through and Port Out would be switched if the positions of Port In and Port Add were exchanged. This result aids in selecting the right ports in device integration.

Some parameters affecting the output spectrum should be carefully selected to optimize the sensing properties of the proposed structure. In this section, the relationship between certain parameters and the output spectra of Port Through are simulated and discussed.

3.1 Phase shift/length of the U-bend waveguide

The length of a light path can be linearly transferred to the light phase, as light signal travels as a wave in the waveguide. Therefore, these two parameters can be discussed together. In the simulation, two phase shifters are used to represent the length change of a light path in the two parts of the bend waveguide. As shown in Fig. 4(a), two phase shifters are added to the two sides of the coupling section between the U-bend and the straight waveguide. In equation $\varphi = kx$, where wave vector $k = 2\pi n/\lambda$ is unchangeable when the light signal and the device material are decided, the light phase φ is proportional to the length of the light path. The length of the light path is equal to the length of the waveguide when dispersion is disregarded. Therefore, the phase shift of the U-bend waveguide can be equivalent to its length. The original length of the U-bend waveguide to meet the condition of interference is set to $2\pi R$, where R is the radius of the nested microring resonator. The spectra with different phase shifts in the two shifters are illustrated in Fig. 4(b). The top and second curves have the same shape, this indicating that the output spectrum is independent of the place where the phase shift occurs or where the waveguide expands. When the phase shift is the integral multiple of π, the output spectra remain unchanged. If the phase shift is π/2, as shown in the third curve in Fig. 4(b), then the FSR of output spectrum is only half of the other spectra. The comparison of the fourth and fifth curves suggests that the output spectra remain a doubled FSR as long as the sum of the phase shift is π. This result is due to the interference of the light signals from the microring and from the U-bend waveguide occurring in the coupling section of the microring and U-bend waveguide. For a certain length of the U-bend waveguide, the destructive interference occurs to depress the dips in a certain wavelength.

Therefore, if the length of the U-bend waveguide is established, then the outcome will be independent of the location of the coupling section between the straight waveguide and the U-bend waveguide.

3.2 Coupling coefficients

As shown in Fig. 1(a), three coupling sections in the proposed structure can be divided into two groups, namely,

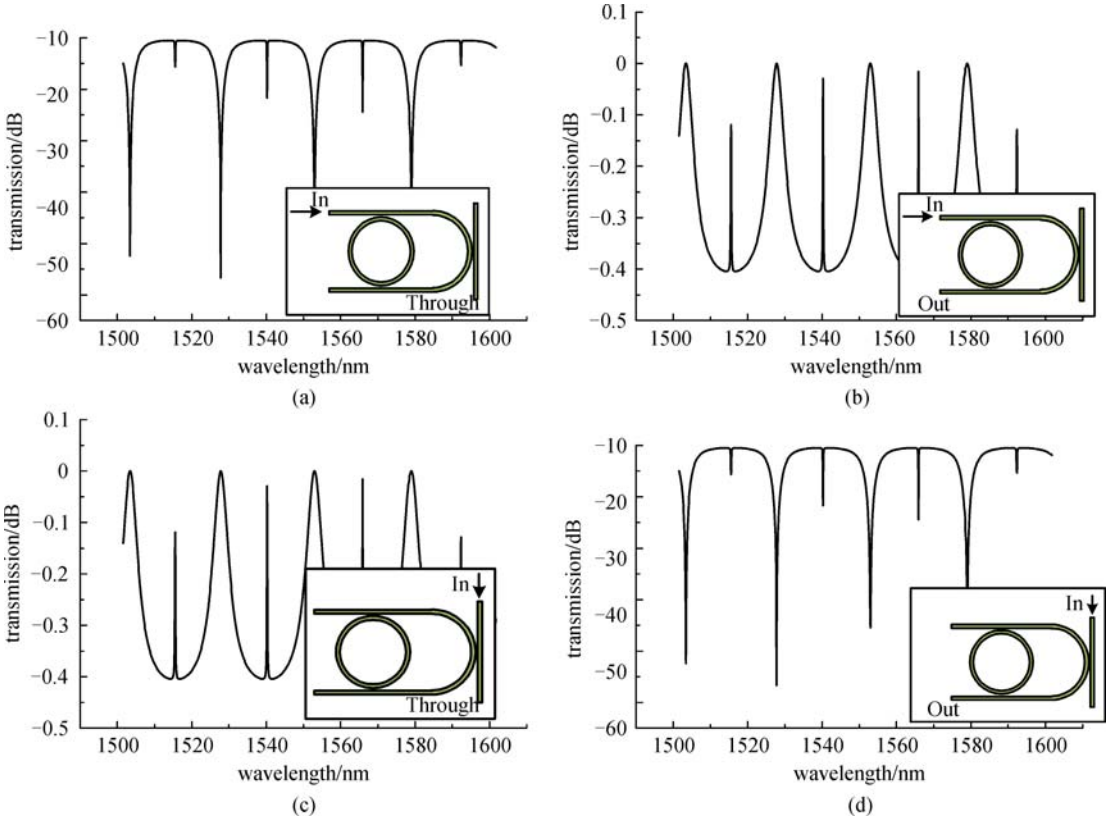

Fig. 3 Output spectra of the proposed structure with different positions for communication: port In and port Through (a) and (d) in different waveguides; (b) and (c) in same waveguide

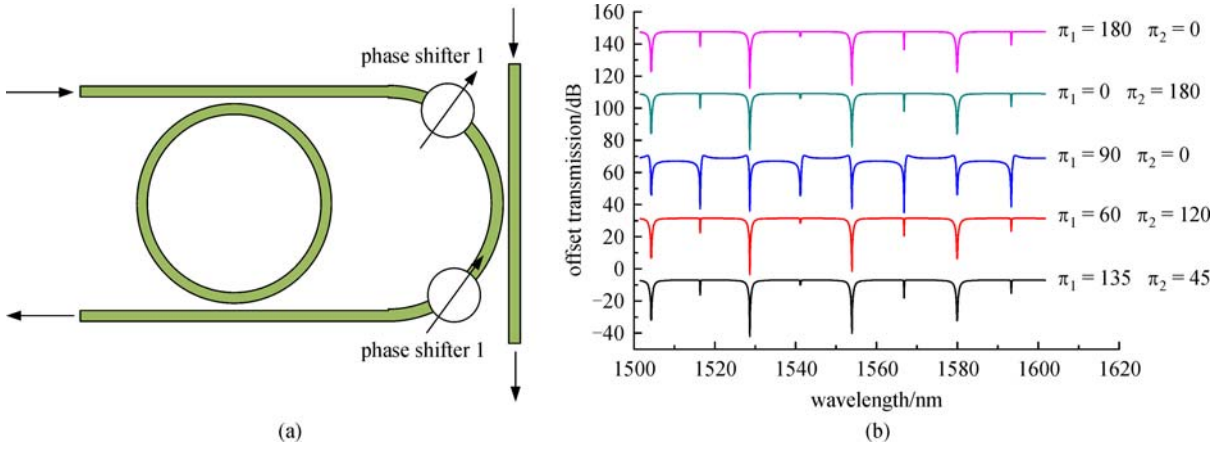

Fig. 4 Output spectra of the proposed structure (a) in different phase shifts (b)

ring-to-waveguide and waveguide-to-waveguide coupling sections. The coupling coefficients of the two groups of coupling sections are discussed in this section. As shown in Fig. 5(a), the coupling coefficient of the ring-to-waveguide sections is maintained at k = 0.2, and the three curves are the output spectra when the coupling coefficients of the waveguide-to-waveguide section are selected as 0.5, 0.2, and 0.05, respectively. When the coupling coefficient of the waveguide-to-waveguide section decreases from 0.5 to 0.05, the basic line level (unfiltered part) decreases from −4 to −14 dB; that is, the transmission loss of the proposed structure increases by 10 dB. While the coupling coefficient of the waveguide-to-waveguide decreases, the pseudo mode is depressed again and the resonant notch is enlarged simultaneously. Consequently, the pseudo-mode depression effect is enhanced by the decrease in coupling coefficient of the waveguide-to-waveguide section. The three curves in Fig.

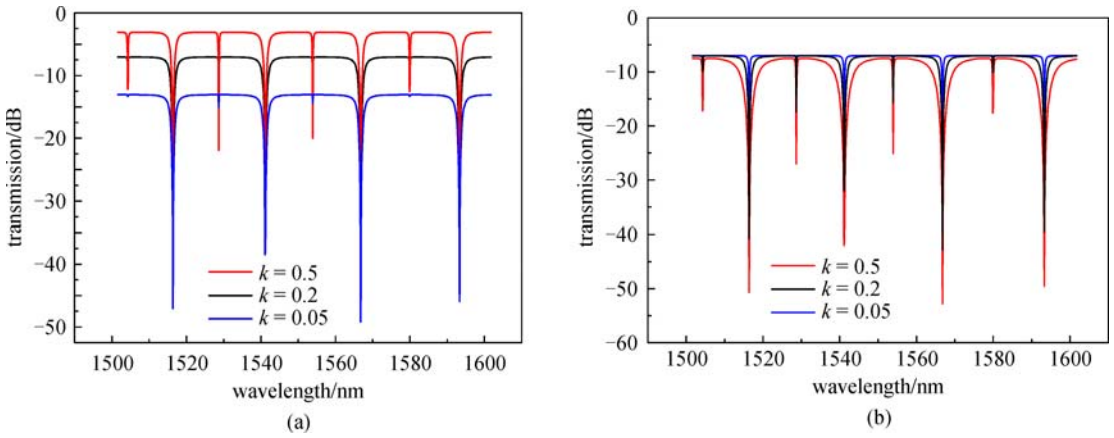

Fig. 5 Output spectra of the proposed structure in the different coupling coefficients. (a) shows the output spectra when the coupling coefficients of the waveguide-to-waveguide section are selected at 0.5, 0.2, and 0.05, respectively, and the coupling coefficient of the ring-to-waveguide sections is maintained at $k = 0.2$; (b) represents the output spectra of Port Through. The coupling coefficient of the waveguide-to-waveguide section is maintained at 0.2, and the coupling coefficients of the ring-to-waveguide are 0.5, 0.2, and 0.05

5(b) are the output spectra of Port Through. The coupling coefficient of the waveguide-to-waveguide section is maintained at 0.2, and those of the ring-to-waveguide are 0.5, 0.2, and 0.05. The bandwidth of the resonant notch is related to the coupling coefficient of the ring-to-waveguide. The resonant notch is considered a pointer in detecting the resonant wavelength shift. Sensor precision can be increased by having a thin pointer. Therefore, the filter outcomes related to sensing properties, such as bandwidth of resonant notch, pseudo-mode depression, and transmission loss, are optimized by the proper selection of the coupling coefficient of the ring-to-waveguide and waveguide-to-waveguide sections.

3.3 Effective index

For optical waveguide sensors, detection is usually based on the variation of an effective refractive index. Therefore, the sensitivity of the refractive index contributes greatly to the sensitivity of the sensor despite the different chemical or physical sensing principles in the waveguide material. The simulation results of the output spectra are shown in Fig. 6. The resonant wavelength redshifts from 1566.8 to 1571.6, and the effective index of the device waveguide increases from 2.2 to 2.2030. Six wavelength redshifts with increasing refractive indices are recorded. As shown in Fig. 7, similar to the conventional single microring structure, redshift data also have a perfect linear property, which proves the suitability of the new structure for sensing applications. In the slope, sensitivity is approximately 6.25×10^{-3} RIU/nm.

The new structure has several advantages compared with the conventional single microring structure in sensing applications. First, the new structure has a larger FSR, that is, a larger measurement range. The proposed structure doubles the FSR under the same radius as that of the conventional ring structure. Second, the ER in the output spectrum of the new structure is enlarged. When the

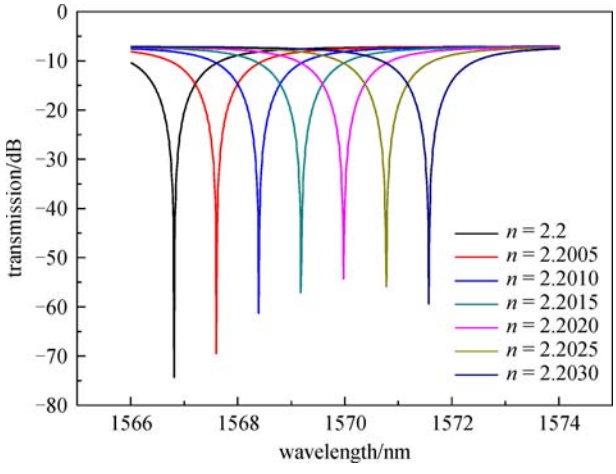

Fig. 6 Redshift of the resonant notch in the output spectrum with increasing n

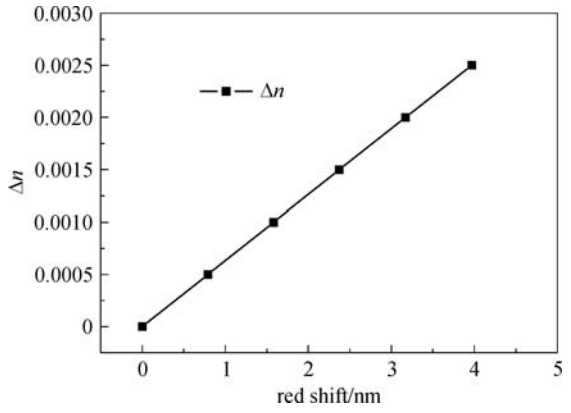

Fig. 7 Sensitivity curve of the sensor

resonant notch of 1567.8 nm is considered as an example, the ER is approximately 68, which is 7 dB larger than that of the conventional structure. A larger ER makes the output signal more obvious. Loss during transmission is inevitably increased by 7 dB to depress the pseud-mode. Third, similar to the add–drop microring resonator, the new structure maintains the linear sensitivity curve. If the material and transverse section of the waveguide in the proposed structure are similar to those of the conventional structure, then the sensitivity curve of the new structure is similar to that of the conventional structure. The positions of the coupling section on the U-bend waveguide and the layout of Port In and Port Out are not correlated with the output spectra.

4 Conclusion

The microring structure with U-bend and straight waveguides proposed in this study can realize both band-reject and band-pass filter spectra. The FSR of the band-reject spectra is verified to double compared with that of the conventional structure. The sensing application parameters, such as ER, pseudo-mode depression, and transmission loss, are optimized through careful parameter selection. This work reports the relationship between the several parameters of the proposed structure and the output filter spectra for sensing applications and provides theoretical direction for micro/nano-optical sensors in the future.

Acknowledgements This study was supported by the National Natural Science Foundation of China (Grant Nos. 61601253 and 61501271) and K. C. Wong Magna Fund in Ningbo University.

References

1. Mi K P, Kee J S, Quah J Y, Netto V, Song J, Fang Q, Fosse E M L, Lo G. Label-free aptamer sensor based on silicon microring resonators. Sensors and Actuators B, Chemical, 2013, 176(6): 552–559
2. Jäger M, Becherer T, Bruns J, Haag R, Petermann K. Antifouling coatings on SOI microring resonators for bio sensing applications. Sensors and Actuators B, Chemical, 2015, 223(4): 400–405
3. Zhao X, Tsai J M, Cai H, Ji X M, Zhou J, Bao M H, Huang Y P, Kwong D L, Liu A Q. A nano-opto-mechanical pressure sensor via ring resonator. Optics Express, 2012, 20(8): 8535–8542
4. Mi G, Horvath C, Aktary M, Van V. Silicon microring refractometric sensor for atmospheric CO_2 gas monitoring. Optics Express, 2016, 24(2): 1773–1780
5. Zang K, Zhang D, Huo Y, Chen X, Lu C Y, Fei E T, Kamins T I, Feng X, Huang Y, Harris J S. Microring bio-chemical sensor with integrated low dark current Ge photodetector. Applied Physics Letters, 2015, 106(10): 101111
6. Mao M, Chen S, Dai D. Cascaded ring-resonators for multi-channel optical sensing with reduced temperature sensitivity. IEEE Photonics Technology Letters, 2016, 28(7): 814–817
7. Zhang C, Chen S, Ling T, Guo L J. Review of imprinted polymer microrings as ultrasound detectors: design, fabrication, and characterization. IEEE Sensors Journal, 2015, 15(6): 3241–3248
8. Prasad P R, Selvaraja S K, Varma M M. High precision measurement of intensity peak shifts in tunable cascaded microring intensity sensors. Optics Letters, 2016, 41(14): 3153–3156
9. Xu Q, Fattal D, Beausoleil R G. Silicon microring resonators with 1.5-microm radius. Optics Express, 2008, 16(6): 4309–4315
10. Lu Y, Fu X, Chu D, Wen W, Yao J. Fano resonance and spectral compression in a ring resonator drop filter with feedback. Optics Communications, 2011, 284(1): 476–479
11. Li Z, Li X, Sun Y, Li S, Zheng W. Doubled free spectral range of single microring resonator filter. Acta Optica Sinica, 2012, 32(7): 224–229
12. Xiang X Y, Wang K R, Yuan J H, Jin B Y, Sang X Z, Yu C X. Highly sensitive digital optical sensor with large measurement range based on the dual-microring resonator with waveguide-coupled feedback. Chinese Physics B, 2014, 23(3): 034206

Xin Zhang received his Ph.D. degree in 2015 from Yanshan University, China. He is a lecturer in the Electrical Engineering and Computer Science Division of Ningbo University. His research field is photonic device and optical gas sensor.

Jiawen Jian received his Ph.D. degree from University of Electronic Science and Technology of China (UESTC). He is a professor in the Electrical Engineering and Computer Science Division of Ningbo University. His research area is electrochemical gas sensor.

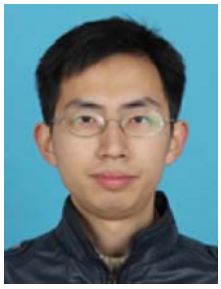

Han Jin received his Ph.D. degree from Kyushu University. He is an associate professor in the Electrical Engineering and Computer Science Division of Ningbo University. His research interests are gas sensor and wearable sensor design.

Peipeng Xu received his Ph.D degree from Zhejiang University. He is lecturer in Laboratory of Infrared Material and Devices in Ningbo University. His research interests are infrared materials and wave-guide design.